

Article

Swelling and Salt Formation in Ibuprofen and Tranexamic Acid-Containing Tablets during High-Temperature Storage

Yuto Kawano ^{1,*}, Yoshiharu Tanaka ¹, Nanami Hata ¹, Yuki Yoshiike ¹, Masato Nakajima ¹, Etsuo Yonemochi ^{2,*} and Nobuhiro Ishihara ¹

¹ R&D Center, Zenyaku Kogyo Co., Ltd., 4-7-1 Minamiosawa, Tokyo 192-0364, Japan

² Department of Physical Chemistry, School of Pharmacy and Pharmaceutical Sciences, Hoshi University, 2-4-41 Ebara, Shinagawa, Tokyo 142-8501, Japan

* Correspondence: yuto_kawano@mail.zenyaku.co.jp (Y.K.); e-yonemochi@hoshi.ac.jp (E.Y.)

Abstract: Ibuprofen (IBP)- and Tranexamic acid (TXA)-containing tablets are known to swell when stored at high temperatures, but the mechanism of swelling is unknown. In this study, we investigated the possible mechanism of swelling with high-temperature storage. Differential scanning calorimetry (DSC) and powder X-ray diffractometry (PXRD) analyses showed that a new complex was formed in swollen tablets, when stored at 50 °C for 60 days. Additionally, we prepared single crystals of IBP and TXA, and analyzed them using single crystal X-ray diffractometry (SCXRD), to identify the new complex formed during storage. This revealed that the single crystal was a salt consisting of IBP and TXA. The PXRD peak of the salt simulated by SCXRD matched that of the PXRD peak of the swollen tablet after storage. These results suggest a close relationship between the swelling and crystal structures of IBP and TXA.



Citation: Kawano, Y.; Tanaka, Y.; Hata, N.; Yoshiike, Y.; Nakajima, M.; Yonemochi, E.; Ishihara, N. Swelling and Salt Formation in Ibuprofen and Tranexamic Acid-Containing Tablets during High-Temperature Storage. *Crystals* **2022**, *12*, 1420. <https://doi.org/10.3390/cryst12101420>

Academic Editors: Duane Choquesillo-Lazarte and Alicia Dominguez-Martin

Received: 27 August 2022

Accepted: 7 October 2022

Published: 8 October 2022

Publisher's Note: MDPI stays neutral with regard to jurisdictional claims in published maps and institutional affiliations.



Copyright: © 2022 by the authors. Licensee MDPI, Basel, Switzerland. This article is an open access article distributed under the terms and conditions of the Creative Commons Attribution (CC BY) license (<https://creativecommons.org/licenses/by/4.0/>).

Keywords: ibuprofen; tranexamic acid; salt; crystal structure; swell

1. Introduction

Ibuprofen (2-(4-Isobutylphenyl)propionic acid, IBP) is a nonsteroidal anti-inflammatory drug that inhibits the activities of cyclooxygenases 1 and 2, which are responsible for the production of prostaglandins. Tranexamic acid (4-(Aminomethyl)cyclohexanecarboxylic acid, TXA), a lysine derivative, suppresses the binding of lysine to plasminogen and exerts anti-plasmin activity. TXA acts as an anti-inflammatory and hemostatic agent, because plasmin increases the production of prostaglandins. Thus, they have completely different modes of action. Therefore, combining IBP and TXA into a single tablet can potentially enhance their anti-inflammatory and antipyretic properties and may be beneficial as an over-the-counter medication. However, solid formulations, such as tablets, of the two drugs can swell under high-temperature conditions, thereby reducing the commercial viability of tablets through cracking [1]. Although many Japanese patents claim methods of preventing the swelling of IBP- and TXA-containing tablets [1–6], the precise mechanism of swelling is not completely understood.

Crystal structure changes, such as salt formation, may affect the shape and size of crystals [7]. Furthermore, a pK_a difference (ΔpK_a) of more than 2 is known to be indicative of salt formation [8]. The ΔpK_a value between IBP ($pK_a(-COOH) = 4.4$) and TXA ($pK_a(-NH_2) = 10.2$) is reported as 5.8 [9,10]. This suggests the possible formation of a salt (IBP–TXA salt). Additionally, it has been reported that the physical mixture (PM) of IBP and nicotinamide transforms into a co-crystal at high temperatures [11]. Hence, IBP can react with other substances under solvent-free conditions, such as in storage. These reports led us to the hypothesis that IBP and TXA may react during high-temperature storage, forming an IBP–TXA salt, which might induce tablet swelling. To evaluate this hypothesis, we analyzed PM containing both IBP and TXA using differential scanning calorimetry (DSC) and powder X-ray diffraction (PXRD), when stored under high-temperature conditions.

Furthermore, the PXRD peak of PM was compared to that of the IBP–TXA salt simulated using single crystal X-ray diffraction (SCXRD).

2. Materials and Methods

2.1. Materials

Powdered IBP and TXA were purchased from Daito Pharmaceutical Co., Ltd. (Toyama, Japan) and Kyowa Pharma Chemical Co., Ltd. (Toyama, Japan). The chemical structures of IBP and TXA are shown in Figure 1.

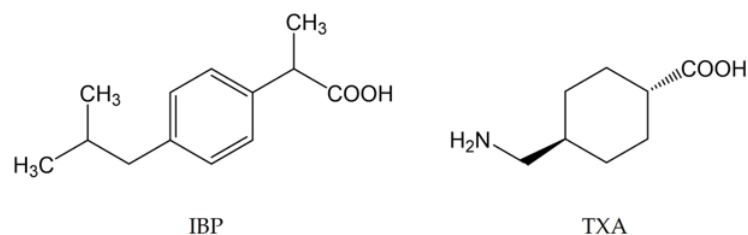


Figure 1. Chemical structures of IBP and TXA.

2.2. Sample Preparation

Powdered PM was prepared by mixing IBP and TXA powders in a 1:2 mass ratio using a mortar and pestle. The PM, IBP, or TXA powders were pressed into tablets using a single punch tableting machine (Riken Yuatu Power; Riken Seiki Co., Ltd., Tokyo, Japan) with flat-face punches, at a pressure of 200 kg/cm². Each tablet had a diameter and weight of 20 mm and 2 g, respectively. A tablet glass bottle of size 5 K, closed with metal caps, and complying with Japanese Industrial Standards was filled with the tablets, IBP, TXA, and PM powders, and maintained at 5 °C, 25 °C, 40 °C, and 50 °C.

A PM solid solution was prepared by melting powdered PM on a hot plate, then heating at a maximum temperature of 330 °C for 10 min, followed by immediate conditioning at 5 °C and rapid cooling.

Single crystals were prepared by dissolving equivalent masses of IBP and TXA in a 50% w/w EtOH solution using a mechanical stirrer. The IBP- and TXA- containing solution was gradually evaporated at 5 °C for one week, and the crystallized products were collected.

2.3. Swelling of Tablet and Morphology of Powder Evaluation

The swelling of the tablets was calculated by the thickness change rate (%), using the following equation:

$$\text{Tablet thickness change rate (\%)} = (T_a - T_b) / T_b \times 100 \quad (1)$$

where T_a and T_b represent the thickness of the tablets after and before storage, respectively.

The data of the tablet thickness change rate were expressed as mean \pm standard division ($n = 3$).

The morphologies of the PM, IBP, and TXA powders, before and after storage at 50 °C for 60 days, were observed under a digital microscope (VHX-5000; Keyence Co., Ltd., Osaka, Japan).

2.4. DSC Analysis

After grinding the tablets, DSC measurements were performed using a DSC-60A (Shimadzu Corp., Kyoto, Japan) under a nitrogen gas flow of 50 mL/min. All samples were heated at 10 °C/min and analyzed from 30 °C to 350 °C.

2.5. PXRD Analysis

After grinding the tablets, PXRD analysis was conducted using a desktop-type powder X-ray diffractometer (MiniFlexII; Rigaku Co., Ltd., Tokyo, Japan) at 30 kV and 15 mA with

a Cu K α radiation source. The samples were scanned from 4° to 40° at a scanning rate of 4/min.

2.6. Attenuated Total Reflectance–Fourier Transform Infrared Spectrometry (ATR-FTIR) Analysis

ATR-FTIR analysis was performed using a Fourier transform infrared spectrometer (Nicolet iS5; Thermo Fisher Scientific Co., Ltd. Tokyo, Japan) in compliance with the Japanese Pharmacopoeia with an ATR accessory (iD7). The samples were analyzed from 1500 cm⁻¹ to 1800 cm⁻¹.

2.7. SCXRD Analysis

A 0.139 × 0.135 × 0.126 mm³ dimensional single crystal was selected from the crystallized products and outsourced to Rigaku Co., Ltd., where structural analysis of the single crystal was performed using a single crystal X-ray diffractometer, XtaLAB Synergy-S (Rigaku Co., Ltd.). X-ray data were collected using the single crystal X-ray data collection and processing software CrysAlis^{Pro} (Rigaku Co., Ltd.) at −173 °C, 50 kV and −1 mA with a Cu K α ($\lambda = 1.54184 \text{ \AA}$) radiation source. Based on the collected X-ray data, the crystal structure was analyzed and refined using the structural analysis program package software Olex2 (OlexSys Ltd., Durham, England). Moreover, data from the crystal structure analysis using the structural analysis program package software Mercury3.1 (The Cambridge Crystallographic Data Centre, CCDC, Cambridge, England) were used to simulate the PXRD pattern. Crystallographic data were deposited at the CCDC, with the number 2202866, and can be obtained via www.ccdc.cam.ac.uk/data_request/cif (accessed on 23 August 2022).

3. Results and Discussion

3.1. Swelling Evaluation

The thickness change rates of the tablets are shown in Figure 2. When PM tablets were stored at 40 °C and 50 °C, they gradually swelled, and after 60 days of storage, their tablet thickness change rates reached 2.96% and 24.9%, respectively. However, there were no differences in the thickness change rates of PM tablets after 60 days of storage at 5 °C (0.25%) and 25 °C (0.06%). Additionally, IBP or TXA tablets did not swell, even when stored at 40 °C and 50 °C, and their thickness change rates ranged from −1.2 to 0.54%. These results confirm that tablets containing both IBP and TXA swell over time at high temperatures.

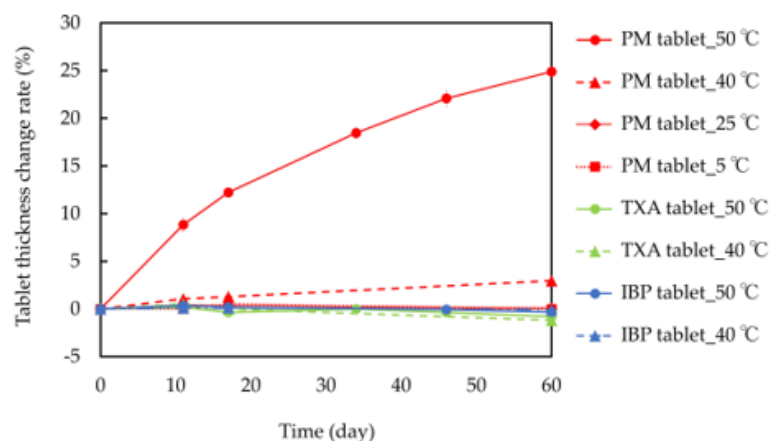


Figure 2. Tablet thickness change rates of IBP, TXA, and PM at 5 °C, 25 °C, 40 °C, and 50 °C for 60 days.

3.2. Crystal Morphology Evaluation

As storage at 50 °C for 60 days clearly induced the swelling of the PM tablets, the morphologies of IBP, TXA, and PM powders after storage were first examined, and the results are shown in Figure 3. Before storage, the crystal morphology of the IBP powder used in this study had a needle-like appearance. Although the crystals were slightly

aggregated with each other, the crystal morphology had not changed after 60 days of storage at 50 °C. Prior to storage, the TXA crystals had a plate-like appearance and wide crystal-size distribution. The crystal morphologies had not changed after 60 days of storage at 50 °C. However, when the PM powder was stored at 50 °C for 60 days, the surface of the IBP crystals with a needle-like structure became rougher than before storage. These results indicate that IBP reacts with TXA during storage at 50 °C.

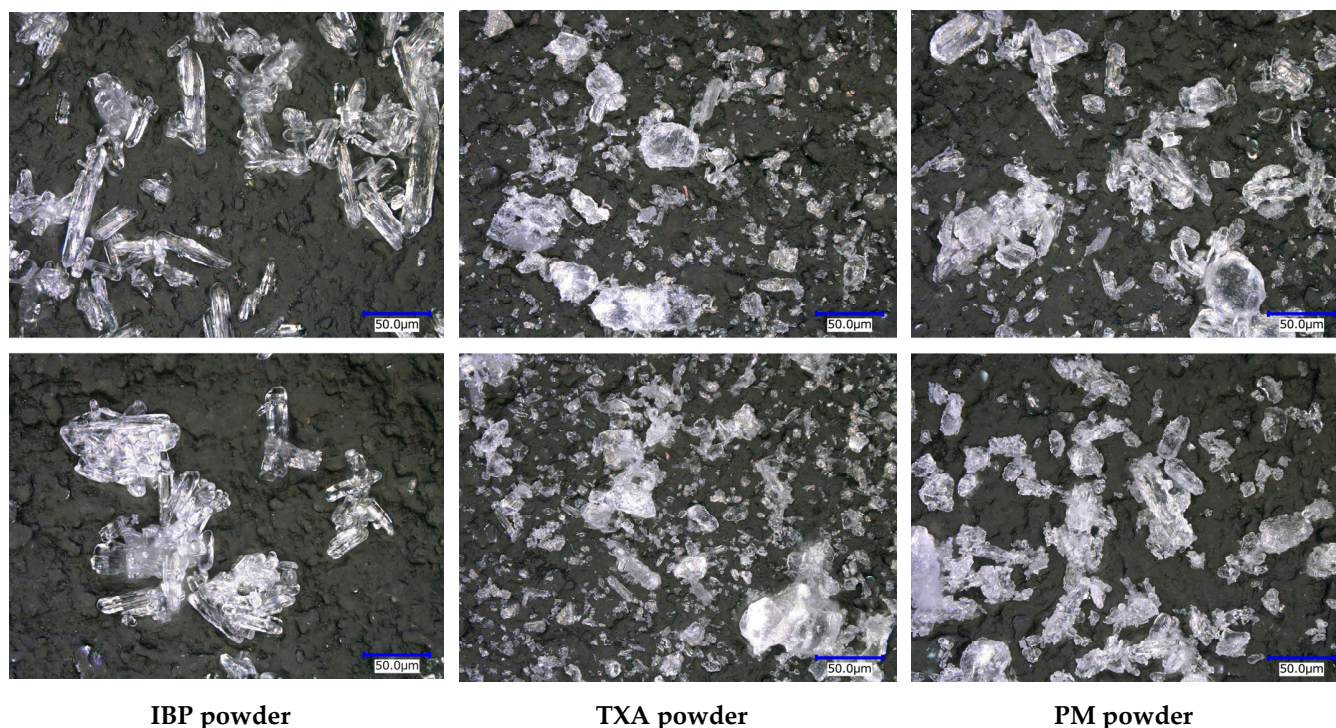


Figure 3. Crystal morphology of the IBP powder, TXA powder, and PM powder before (**above**) and after (**below**) storage at 50 °C for 60 days.

3.3. DSC Analysis

The thermograms, endothermic temperature, and energy amount of the IBP and TXA tablets, PM powder, PM tablet, and PM solid solution at approximately 75 °C and 180 °C are shown in Figure 4 and Table 1. A new endothermic reaction was observed at approximately 180 °C in the PM powder and PM tablet, which tended to increase with the storage temperature. However, the endothermic reaction in the PM tablet tended to decrease at approximately 75 °C. These results show that a new complex between IBP and TXA was formed, and high-temperature storage could induce the formation of this complex. In this study, a new peak also appeared before storage. A baseline shift, which was considered an exothermic reaction, was observed after the melting point of IBP. Thus, this peak was considered to result from a new complex formed by the reaction of melting IBP and non-melting TXA. Additionally, almost no difference in melting points was observed between the complex formed with storage at 50 °C for 60 days and the complex formed by the reaction of melting IBP and non-melting TXA. These results suggest that the complex formed during storage and measurement may have been the same substance. Next, a PM solid solution was prepared and evaluated because IBP and TXA could form a complex when heated. However, the PM solid solution did not show endothermic or exothermic reactions. The PM solid solution was quickly prepared by quenching; thus, it may not have been fully crystallized, resulting in an amorphous state.

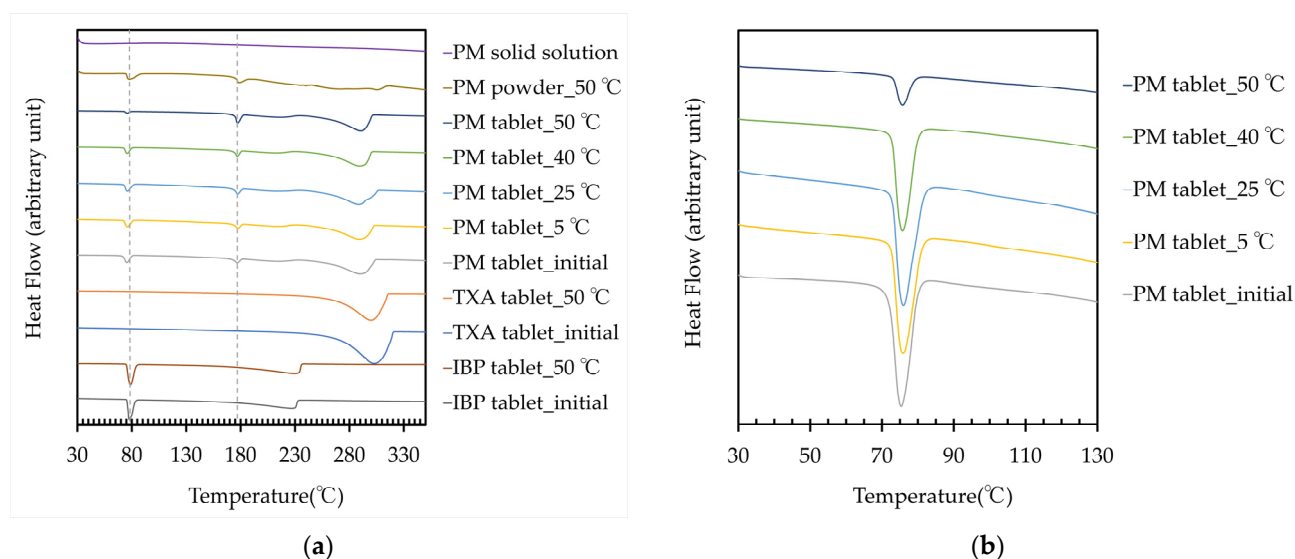


Figure 4. (a) Thermograms of the IBP, TXA, and PM tablets before and after storage for 60 days, PM powder, and PM solid solution; (b) Thermogram of the PM tablet at approximately 75 °C, before and after storage for 60 days.

Table 1. Endothermic temperatures and energy amount associated with IBP and newly formed complexes, before and after storage for 60 days, and PM solid solution.

Sample	Melting Point of IBP (°C)	Endothermic Energy Amount around 75 °C (J/g)	Endothermic Temperature around 180 °C (°C)	Endothermic Energy Amount around 180 °C (J/g)
IBP tablet_initial	77.79	119.47	-	-
IBP tablet_50 °C	78.68	125.69	-	-
TXA tablet_initial	-	-	-	-
TXA tablet_50 °C	-	-	-	-
PM tablet_initial	76.93	44.57	173.89	11.87
PM tablet_5 °C	75.85	36.49	177.41	27.29
PM tablet_25 °C	75.99	37.33	177.23	31.34
PM tablet_40 °C	75.74	28.02	176.88	29.31
PM tablet_50 °C	75.70	5.66	177.23	37.86
PM powder_50 °C	77.75	24.72	178.64	20.37
PM solid solution	-	-	-	-

3.4. PXRD Analysis

The PXRD patterns of the IBP, TXA, PM tablets, and PM solid solution are shown in Figure 5. Although storage did not affect the PXRD patterns of the IBP or TXA tablets, a new peak of PXRD appeared at 8.5° in the diffractogram of the PM tablet after storage at 50 °C for 60 days. The appearance of this peak depended on the temperature. The intensity of this peak was weak in the PM tablet after storage at 40 °C for 60 days, while after storage at 25 °C or 5 °C for 60 days, the peak is virtually undetectable. Moreover, a new peak at approximately 8.5° was also detected in the diffractogram of the PM powder (8.8°) when stored at 50 °C for 60 days. The DSC and PXRD analyses indicated that a new complex was formed when the tablets were stored at high temperature. Furthermore, the IBP-derived peak of PM around 16.8° decreased after storage, and had nearly vanished after storage at 50 °C. This result indicates that the PM was TXA-rich, at a 1:2 mass ratio of complex formation, as the peak in the PM stored at 50 °C almost had disappeared for free IBP, i.e., IBP that does not form a complex. Additionally, the PXRD pattern of the PM solid solution differed from that of PM, and did not exhibit a peak near 8.5°. This result indicates that the rapid cooling and short preparation time may have affected the crystalline state.

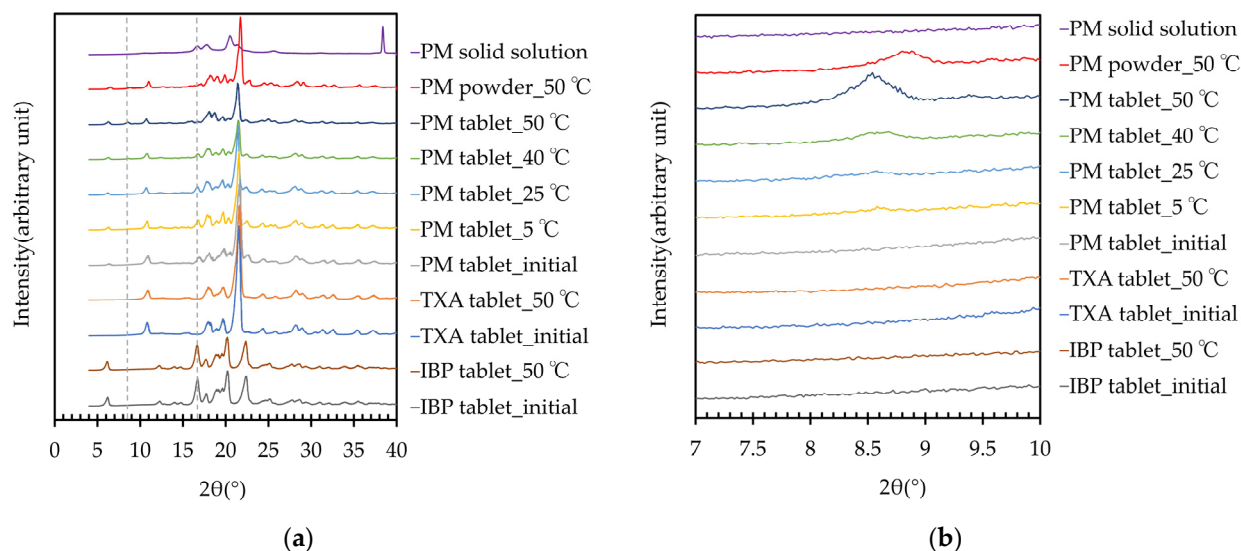


Figure 5. (a) PXRD patterns of IBP, TXA, and PM before and after storage for 2 months, and PM solid solution; (b) PXRD peaks of IBP, TXA, PM, and PM solid solution around 8.5° – 8.8° , before and after storage for 60 days.

3.5. ATR-FTIR Analysis

The ATR-FTIR spectra of IBP, TXA, PM, PM solid solution, and single crystal are shown in Figure 6. In the PM solid solution, the peaks of TXA-derived carbonyl groups around 1530 cm^{-1} and IBP-derived carbonyl groups around 1710 cm^{-1} are shifted [10,12]. This indicates that the PM solid solution may interact between the carbonyl groups of IBP and TXA. Next, a single crystal composed of IBP and TXA was produced and evaluated. In the single crystal, the peak of the carbonyl group of TXA around 1530 cm^{-1} and the amino group of TXA around 1640 cm^{-1} is shifted [12]. The difference between the ATR-FTIR spectra of the PM solid solutions and single crystals can be attributed to the incomplete crystallization of the PM solid solutions. As the DSC and PXRD results suggest that IBP and TXA form a complex, the single crystal may be a novel complex composed of IBP and TXA.

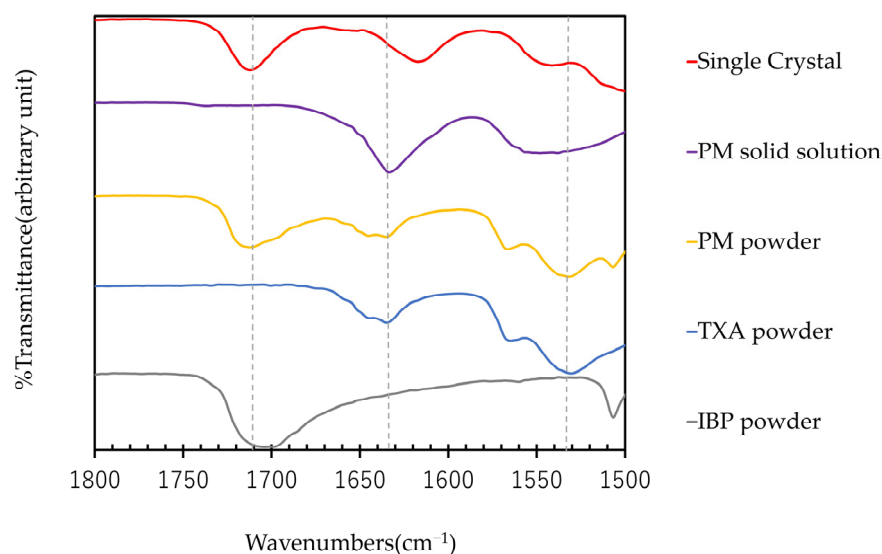


Figure 6. ATR-FTIR spectra of IBP, TXA, PM, PM solid solution, and single crystal.

3.6. SCXRD Analysis

First, an SCXRD analysis was performed on single crystals selected from the crystallized products, to confirm the formation of the IBP–TXA salt. As the protons from the carbonyl group of IBP are transferred to the amino group of the aliphatic (cyclic) primary amine of TXA, the single crystal selected was an IBP–TXA salt (Figure 7). Furthermore, the IBP–TXA salt contains one molecule each of IBP and TXA in the asymmetric unit, in a 1:1 molar ratio.

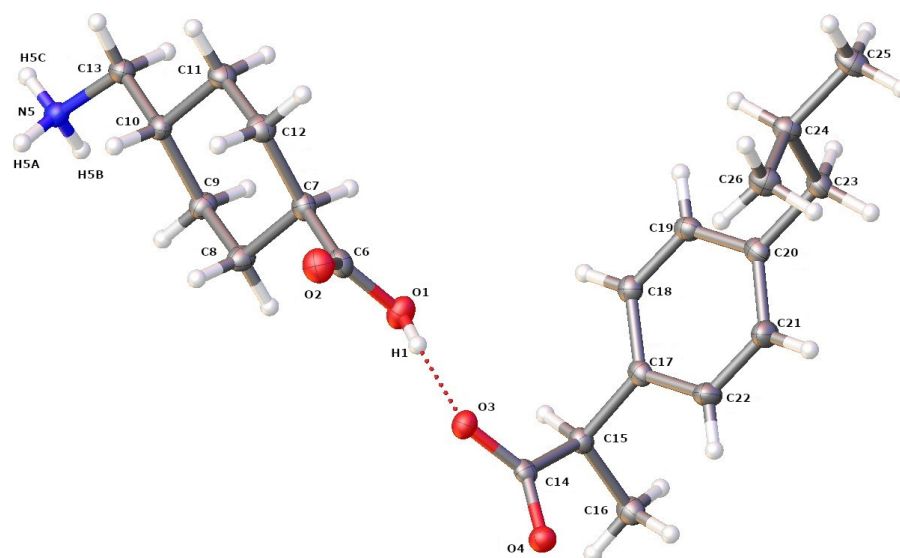


Figure 7. ORTEP diagram of IBP and TXA in salt showing the atom numbering scheme. The hydrogen atoms are shown as small white spheres with arbitrary radii.

The crystallographic information, geometrical parameters for the hydrogen bonding interaction, and molecular states in the crystal unit lattice are summarized in Tables 2 and 3 and Figure 8. The crystal unit lattice has four molecules of IBP–TXA salt. All four molecules of IBP in the crystal unit lattice are regularly arranged in the center. Additionally, the TXA molecules are regularly arranged outside IBP in both molecules. Moreover, the IBP–TXA salt has one hydrogen bond between the carbonyl groups of IBP and TXA and three hydrogen bonds between the carbonyl groups of IBP and the amino group of TXA. Therefore, the difference between the ATR-FTIR spectra of PM and single crystals can be attributed to the bonds of the carbonyl and amino groups of TXA.

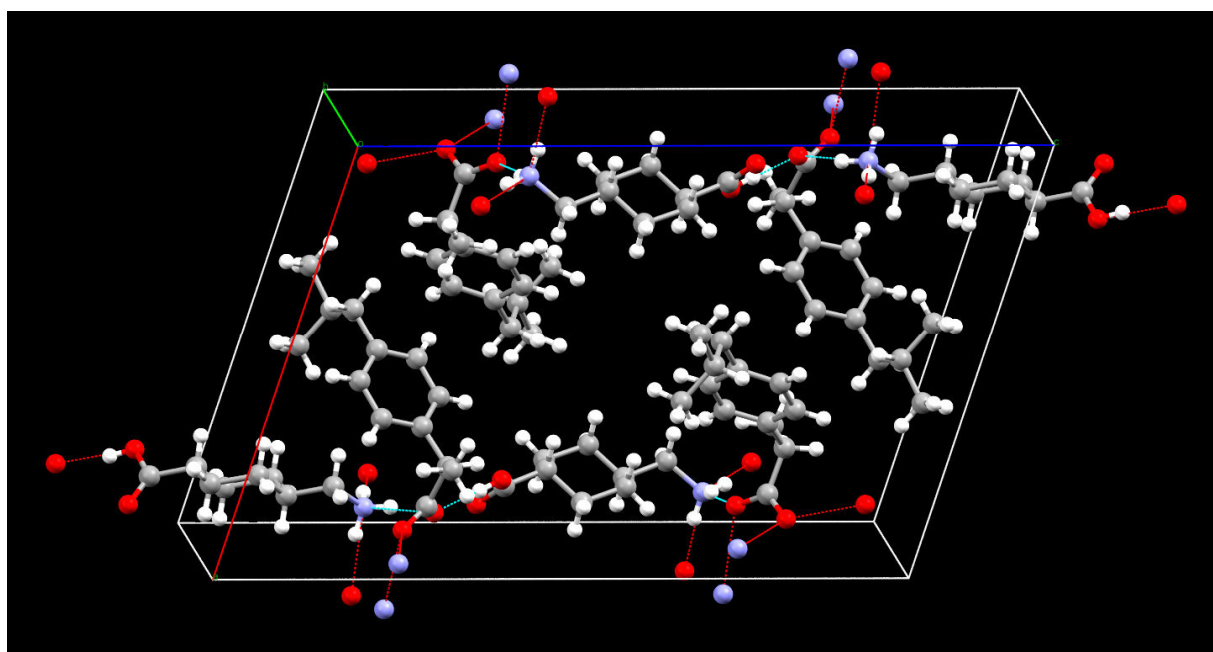
Next, the XRD pattern of the IBP–TXA salt was simulated using the data obtained from the SCXRD analysis, as shown in Figure 9. Peaks with high intensities were observed at 6.3° , 8.4° , 16.2° , 18.5° , 19.1° , 21.1° , and 25.6° . Among these, the peaks at 6.3° , 16.2° , 18.5° , and 19.1° were also observed in the PXRD pattern of the IBP tablet, while the peaks at 21.1° and 25.6° were also observed in the PXRD pattern of the TXA tablet (Figure 5). However, neither the IBP nor the TXA tablets showed the simulated PXRD peak at 8.4° . These results indicate that the newly formed complex may be IBP–TXA salt, despite minor differences in the peak positions between the salt (8.4°) and PM tablets (8.5°) stored at 40°C and 50°C for 60 days. These differences are speculated to be due to the influence of IBP and TXA, which does not contribute to salt formation in the PM tablet.

Table 2. Crystallographic data for the IBP–TXA salt.

Parameters	IBP–TXA Salt
Molecular formula	C ₂₁ H ₃₃ NO ₄
Molecular weight	363.48
Temperature (K)	100.00(10)
Crystal system	Monoclinic
Space group	P2 ₁ /c
Lattice parameters (Å, °)	a = 14.4682(3), α = 90 b = 6.60510(10), β = 105.894(2) c = 21.8870(4), γ = 90
Volume(Å ³)	2011.64(7)
Z	4
D _{calcd} (Mg/m ³)	1.200
Absorption coefficient (mm ⁻¹)	0.656
F (000)	792.0
Theta range for data collection (°)	6.352 to 155.006
Index ranges	−18 ≤ h ≤ 18, −8 ≤ k ≤ 8, −19 ≤ l ≤ 26
Reflections collected	39,241
Independent reflections	4236 [R _{int} = 0.0294, R _{sigma} = 0.0135]
Data/restraints/parameters	4236/0/241
Goodness-of-fit on F ²	1.042
Final R indexes [I ≥ 2σ (I)]	R1 = 0.0335, wR2 = 0.0859
Final R indexes [all data]	R1 = 0.0345, wR2 = 0.0870
Largest diff. peak and hole (e Å ³)	0.30/−0.19

Table 3. Geometrical parameters of the hydrogen bonding interaction in the IBP–TXA salt.

D-H ⋯ A	D-H (Å)	H-A (Å)	D-A (Å)	D-H ⋯ A (°)
O1-H1 ⋯ O3	0.82	1.82	2.6293(10)	170.4
N5-H5A ⋯ O4 ¹	0.89	1.91	2.7734(11)	163.3
N5-H5B ⋯ O4 ²	0.89	1.95	2.8216(11)	165.8
N5-H5C ⋯ O3 ³	0.89	1.96	2.7913(11)	155.0

**Figure 8.** Packing diagram of the IBP–TXA salt (red: oxygen, blue: nitrogen, grey: carbon, white: hydrogen).

Finally, we determined whether the crystal volumes changed before and after salt formation. The crystal unit cell of the IBP–TXA salt consists of four molecules each of IBP and TXA, with a volume of 2011.64 \AA^3 (Tables 2 and 3, Figure 8). However, the crystal unit cell of IBP or TXA alone constitutes four molecules each by volume data, with Final R indexes $<7\%$ from the crystal structure data deposited at CCDC, and the volume ranges of 1162.89 to 1226.38 \AA^3 and 816.19 to 828.16 \AA^3 , respectively [13–17]. Therefore, the total volume of the crystal unit cells of IBP and TXA is similar to that of the IBP–TXA salt. Therefore, the mechanism of tablet swelling cannot be described by the volume of the crystal unit cell. However, the tablets are considered to swell, owing to the changes in the physicochemical properties of the IBP or TXA powders during the formation of the IBP–TXA salt, as the swelled tablets may consist of a mixture of IBP, TXA powders, and IBP–TXA salt. The generated gas is also known to cause swelling, and the sublimation of IBP significantly increases when stored together with TXA [18,19]. Therefore, sublimated IBP is considered as one of the causes of the swelling of PM.

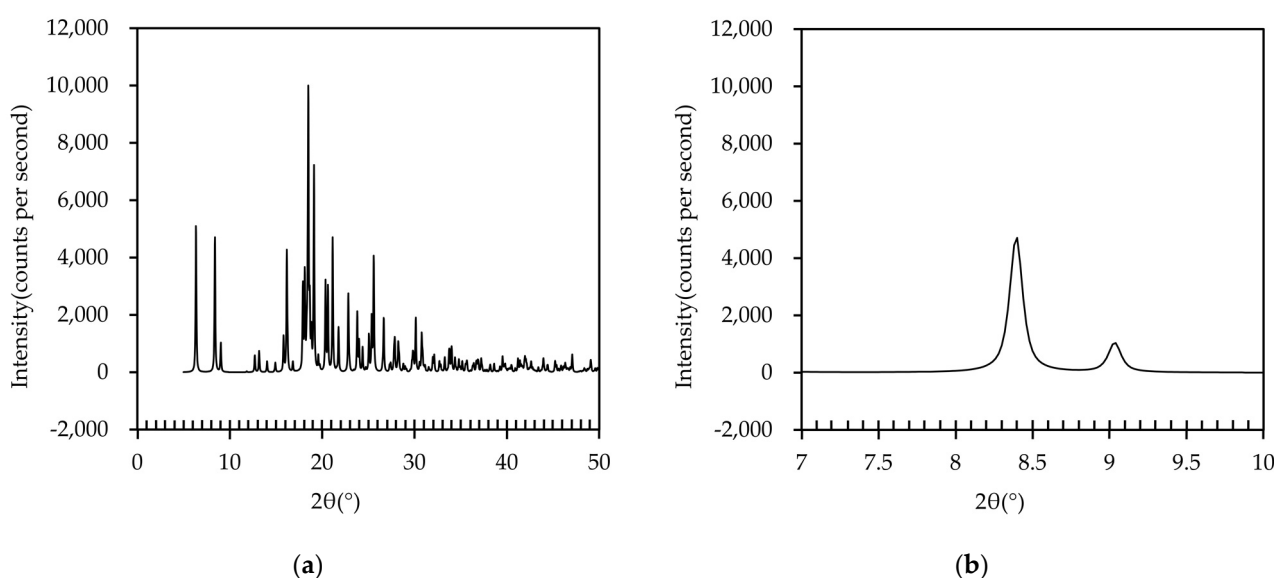


Figure 9. (a) PXRD pattern of IBP–TXA salt; (b) PXRD peak of IBP–TXA salt near 8.5° .

4. Conclusions

Combination therapy with IBP and TXA is expected to enhance their anti-inflammatory and antipyretic properties. However, obstacles such as the swelling of these over-the-counter medications containing both IBP and TXA during high-temperature storage have not been fully overcome. In this study, we found that IBP and TXA form a salt, and confirmed that storage of IBP and TXA at high temperatures may induce salt formation, thereby causing the tablets to swell (Figure 10).

Our research also highlights the importance of developing methods to inhibit salt formation, which could be used to develop IBP- and TXA-containing tablets as over-the-counter drugs with anti-inflammatory and antipyretic properties.

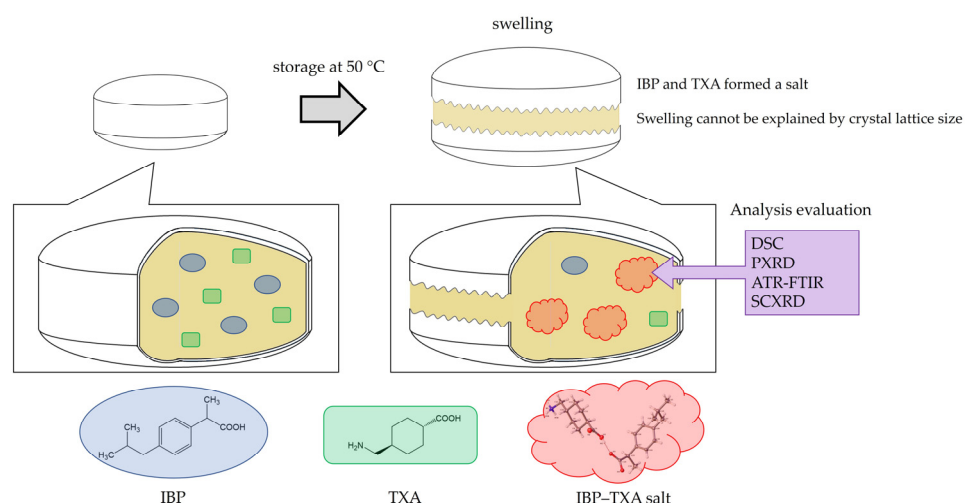


Figure 10. Swelling and salt formation in ibuprofen and tranexamic acid-containing tablets.

Author Contributions: Conceptualization, Y.K.; validation, Y.K., Y.Y. and M.N.; investigation, Y.K.; data curation, Y.K.; writing—original draft preparation, Y.K.; writing—review and editing, Y.T., N.I. and E.Y.; visualization, Y.K. and N.H.; supervision, Y.T. and N.I. All authors have read and agreed to the published version of the manuscript.

Funding: This research received no external funding.

Data Availability Statement: The raw data in Section 3.6 of the manuscript are available in CCDC as CCDC numbers 2202866.

Acknowledgments: The authors thank the CCDC for allowing the use of the deposited crystal data. The authors would like to thank Kazuhiko Haruta, Mika Bunko, and Kayoko Okada from Zenyaku Kogyo Co., Ltd. for providing useful advice on editing this paper.

Conflicts of Interest: The authors declare no conflict of interest.

References

1. Takahara, S.; Nishi, A. Film Coating Tablet. International Patent Application No. JP2019019128A, 5 September 2022.
2. Kano, Y. Solid Preparation Comprising Ibuprofen and Tranexamic Acid. WIPO (PCT) International Patent Application No. WO2008044331A1, 4 October 2007.
3. Yoshikawa, T.; Matsuoka, A.; Matoba, H. Stabilized Pharmaceutical Formulation. International Patent Application No. JP2007145758B2, 19 December 2012.
4. Usui, T.; Shimokawa, T.; Kawashima, H. Solid Preparation Containing Ibuprofen and Tranexamic Acid. International Patent Application No. JP2009203218B2, 15 October 2009.
5. Noritaka, I.; Tsunoda, K.; Ishida, K. Pharmaceutical Preparation and Method for Producing the Same. International Patent Application No. JP2007284423B2, 9 April 2014.
6. Usui, T. Solid Preparation Containing Ibuprofen, Tranexamic Acid and Calcium Silicate. International Patent Application No. JP2010030903B2, 12 February 2010.
7. Falini, G.; Fermani, S.; Tosi, G.; Dinelli, E. Calcium Carbonate Morphology and Structure in the Presence of Seawater Ions and Humic Acids. *Cryst. Growth Des.* **2009**, *9*, 2065–2072. [[CrossRef](#)]
8. Childs, S.L.; Stahly, G.P.; Park, A. The Salt–Cocrystal Continuum: The Influence of Crystal Structure on Ionization State. *Mol. Pharm.* **2007**, *4*, 323–338. [[CrossRef](#)] [[PubMed](#)]
9. Shaw, L.R.; Irwin, W.J.; Grattan, T.J.; Conway, B. The Effect of Selected Water-Soluble Excipients on the Dissolution of Paracetamol and Ibuprofen. *Drug Dev. Ind. Pharm.* **2005**, *31*, 515–525. [[CrossRef](#)] [[PubMed](#)]
10. Nechipadappu, S.K.; Reddy, I.R.; Tarafder, K.; Trivedi, D.R. Salt/Cocrystal of Anti-Fibrinolytic Hemostatic Drug Tranexamic acid: Structural, DFT, and Stability Study of Salt/Cocrystal with GRAS Molecules. *Cryst. Growth Des.* **2018**, *19*, 347–361. [[CrossRef](#)]
11. Ishihara, S.; Hattori, Y.; Otsuka, M.; Sasaki, T. Cocrystal Formation through Solid-State Reaction between Ibuprofen and Nicotinamide Revealed Using THz and IR Spectroscopy with Multivariate Analysis. *Crystals* **2020**, *10*, 760. [[CrossRef](#)]
12. Toledo, M.V.; José, C.; Suster, C.R.L.; Collins, S.E.; Portela, R.; Bañares, M.A.; Briand, L.E. Catalytic and molecular insights of the esterification of ibuprofen and ketoprofen with glycerol. *Mol. Catal.* **2021**, *513*, 111811. [[CrossRef](#)]
13. Shankland, N.; Wilson, C.C.; Florence, A.; Cox, P.J. Refinement of Ibuprofen at 100K by Single-Crystal Pulsed Neutron Diffraction. *Acta Crystallogr. Sect. C Cryst. Struct. Commun.* **1997**, *53*, 951–954. [[CrossRef](#)]

14. Ostrowska, K.; Kropidłowska, M.; Katrusiak, A. High-Pressure Crystallization and Structural Transformations in Compressed R,S-Ibuprofen. *Cryst. Growth Des.* **2015**, *15*, 1512–1517. [[CrossRef](#)]
15. Kleemiss, F.; Justies, A.; Duvinage, D.; Watermann, P.; Ehrke, E.; Sugimoto, K.; Fugel, M.; Malaspina, L.A.; Dittmer, A.; Kleemiss, T.; et al. Sila-Ibuprofen. *J. Med. Chem.* **2020**, *63*, 12614–12622. [[CrossRef](#)] [[PubMed](#)]
16. Groth, P.; Rasmussen, S.E.; Taylor, D.B.; Haug, A.; Enzell, C.; Francis, G. Crystal Structure of the trans Form of 1,4-Aminomethylcyclohexanecarboxylic Acid. *Acta Chem. Scand.* **1968**, *22*, 143–158. [[CrossRef](#)] [[PubMed](#)]
17. Shahzadi, S.; Ali, S.; Parvez, M.; Badshah, A.; Ahmed, E.; Malik, A. Synthesis, spectroscopy and antimicrobial activity of vanadium(III) and vanadium(IV) complexes involving Schiff bases derived from Tranexamic acid and X-ray structure of zwitter ion of Tranexamic acid. *Russ. J. Inorg. Chem.* **2007**, *52*, 386–393. [[CrossRef](#)]
18. Lin, Y.-J.; Hwang, K.-S. Swelling of Copper Powders during Sintering of Heat Pipes in Hydrogen-Containing Atmospheres. *Mater. Trans.* **2010**, *51*, 2251–2258. [[CrossRef](#)]
19. Usui, T. Ibuprofen-Containing Preparation Suppressed in Ibuprofen Sublimation. International Patent Application No. JP2008201738A, 4 September 2008.